Am J Transl Res 2021;13(4):2296-2307
www.ajtr.org /ISSN:1943-8141/AJTR0114354

*Original Article*

# Peroxisome proliferator-activated receptor γ improves pemetrexed therapeutic efficacy in non-squamous non-small cell lung cancer

Tianxing Hang[1,2*], Li Yang[3*], Xiujuan Zhang[1*], Jing Li[1*], Feng Long[1*], Ning Zhu[1*], Ying Li[4], Jingwen Xia[1], Youzhi Zhang[1], Peng Zhang[1], Yuanyuan Zhang[1], Xiaomin Wei[1], Shengqing Li[1]

*[1]Department of Pulmonary and Critical Care Medicine, Huashan Hospital, Fudan University, Shanghai, China; [2]Department of Tuberculosis, The Second Hospital of Nanjing, Nanjing University of Chinese Medicine, Nanjing, China; [3]Department of Anesthesiology, Changzheng Hospital, Navy Medical University of Chinese PLA, Shanghai, China; [4]Department of Respiratory Medicine, Shaanxi Provincial Second People's Hospital, Xi'an, China. [*]Equal contributors.*

Received May 14, 2020; Accepted January 20, 2021; Epub April 15, 2021; Published April 30, 2021

**Abstract:** Objective: The folic acid analog pemetrexed (PMX) is recommended for the first-line chemotherapy for advanced non-squamous non-small cell lung cancer (NSCLC). However, the mechanisms underlying PMX cytotoxicity in NSCLC remain to be fully explored. Methods: PMX effect was evaluated in a urethane-induced lung adenocarcinoma mouse model. The interaction between PMX and intracellular proteins, particularly peroxisome proliferator-activated receptor γ (PPARγ), was investigated. The role of PPARγ in mediating pemetrexed cytotoxicity was investigated using NSCLC cell lines, mouse models and clinical specimens. Results: This study found that PPARγ expression was correlated with prolonged progression-free survival in NSCLC patients. PPARγ downregulated hypoxanthine-guanine phosphoribosyl transferase (HGPRT), a key enzyme for nucleotide salvage synthesis, thereby sensitizing cells to PMX inhibition on nucleotide de novo synthesis. PMX was also a candidate partial agonist of PPARγ, and PMX-activated PPARγ bound to NF-κB and transcriptionally suppressed the NF-κB target gene, *c-Myc*. PMX inhibited tumor growth by activating PPARγ in a urethane-induced lung cancer model characterized by elevated NF-κB activity. Conclusion: PPARγ improves pemetrexed therapeutic efficacy in non-squamous NSCLC. The cytotoxicity effect of PMX can be synergized by activating PPARγ and thereby inhibiting NF-κB pathway.

**Keywords:** Peroxisome proliferator-activated receptor γ, pemetrexed, non-squamous non-small cell lung cancer, NF-κB, hypoxanthine-guanine phosphoribosyl transferase

## Introduction

Lung cancer is the most common cause of cancer-related mortality in humans [1]. Lung cancer can be histologically classified as small cell lung cancer (SCLC), squamous cell cancer and non-squamous non-small cell lung cancer (NSCLC) [2]. The last two decades have witnessed the remarkable advances in the therapeutic regimens of lung cancer, which were represented by molecular targeted therapy and immunotherapy. However, chemotherapy, surgery and radiotherapy are still the basis in the treatment of lung cancer. Chemotherapy is the essential treatment for the patients who are unsuitable for surgery [3].

Pemetrexed (PMX), a folic acid antagonist recommended for the first-line chemotherapy for advanced non-squamous NSCLC, has significantly shifted the expectations for clinical outcomes [4]. Bioactivity tests have indicated that PMX inhibits at least three folate-dependent enzymes, including thymidylate synthase (TYMS), dihydrofolate reductase (DHFR), and glycinamide ribonucleotide formyl transferase (GARFT) [5]. These enzymes play an active role in the synthesis of purine and pyrimidine, and subsequently the formation of ribonucleic acid (RNA) and deoxyribonucleic acid (DNA), which are essential for the survival and division of cancer cells [6]. These studies did not rule out the probability that PMX also suppressed

NSCLC via the mechanism yet to be unraveled [7]. Despite of the adverse events as exemplified by low blood cell counts and mental fatigue, PMX is also used for the maintenance therapy in lung cancer without cumulative toxicity over a prolonged period of time [8]. However, the predictive biomarkers of NSCLC response to PMX remain undetermined [9]. This study aimed to identify the potential proteins that may play a regulatory role in the susceptibility to PMX and to explore how they mediate the therapeutic efficacy of PMX in NSCLC.

PPARγ is a nuclear receptor protein that regulates the expression of genes involved in metabolism and catabolism [10]. PPARγ has been shown to upregulate adenylosuccinate synthase (ADSS) and phosphoribosyl pyrophosphate synthetase 1 (PRPS1), both of which are involved in purine nucleotide metabolism [11]. Recent epidemiological studies have indicated that PPARγ was a potential target for lung cancer chemoprevention [12, 13]; PPARγ and its agonists thiazolidinediones (TZDs) counteracted proliferation and metastasis, and promoted apoptosis of NSCLC cells [14]. X-ray crystallography data further revealed that TZDs (full agonists, e.g. rosiglitazone) activated PPARγ through direct interaction with its transactivation region AF-2 in the Y-shaped ligand-binding domain (LBD). In addition to TZDs, partial agonists of PPARγ [e.g., (2S)-2-(biphenyl-4-yloxy)-3-phenylpropanoic acid], which do not bind to AF-2, are developed to avoid cardiovascular side effects of full agonists [16, 17]. In this article, the relationship between the level of PPARγ and the therapeutic efficacy of PMX was investigated in non-squamous NSCLC patients, and the molecular mechanism of PPARγ in enhancing the efficacy of PMX was further explored. It is concluded that PPARγ can be used as a potential predictive biomarker for PMX treatment of lung cancer.

## Materials and methods

### *Patients*

Forty-four non-squamous NSCLC patients (aged 18-80 years) who systematically received the first-line PMX-based chemotherapy between January 2012 and January 2016 in Huashan Hospital Fudan University were retrospectively enrolled and analyzed. All the patients were histologically diagnosed as advanced (stage III/IV) non-squamous NSCLC or recurrent disease, and could provide target lesions for assessment by RECIST v1.0 criteria and sufficient lung cancer tissue samples for further study. The exclusion criteria included a history of other malignant diseases and no survival data available. Kaplan-Meier analysis was used to identify the difference in the progression-free survival between high and low PPARγ expression groups. This study was approved by the ethics committee of Huashan Hospital Fudan University, and the informed consent was obtained from all the participants.

### *Cell lines and reagents*

The immortalized bronchial epithelial cell line BEAS-2B and human lung cancer cell line A549, H520, SW900, H2170 and PC-9 were purchased from ATCC (Manassas, USA). The human lung cancer SPCA-1 cell line was obtained from the Cell Bank of Shanghai Institute for Biological Sciences, Chinese Academy of Sciences. All the cell lines were characterized by gene profiling by the providers, and were propagated and frozen for future study after receipt. Cells were cultured in RPMI 1640 or DMEM medium supplemented with 10% fetal bovine serum (FBS) and maintained at 37°C in a humidified incubator with 5% $CO_2$. The cultures were split at 90% confluence, and the media were changed once every 2 days. PMX was obtained from Eli Lilly Japan K.K. (Hyogo, Japan) and diluted with phosphate-buffered saline (PBS). GW9662 was purchased from Cayman Chemical.

### *Cell proliferation assay*

The relative cell proliferation was analyzed using commercially available CCK-8 Kit (Dojindo, Shanghai, China) according to the manufacturer's instruction. Briefly, cells were seeded into 96-well plates and subject to different treatments. 10 μl CCK-8 solution was added to each well and incubated at 37°C for 1-4 h, depending on chromogenic reaction. The relative absorbance was determined at 450 nm using a plate reader (Bio-RAD, Hercules, USA).

### *Western blotting*

The total proteins of cells and tissues were harvested with radio immunoprecipitation assay buffer (RIPA, Invitrogen, Carlsbad, USA) containing proteinase inhibitors. After separation in the sodium dodecyl sulfate polyacrylamide

gel electrophoresis (SDS-PAGE), the protein was transferred into polyvinylidene fluoride (PVDF) membranes. The membranes were blocked with 5% BSA in TBST and then incubated overnight (4°C) with primary antibodies against PPARγ, phosphorylated p65, p65, c-Myc, HGPRT, or β-actin (Cell Signaling Technology, Boston, USA). An HRP-conjugated secondary antibody (DAKO, Glostrup, Denmark) was used to identify the primary antibodies. The blots were visualized by ECL detection (Invitrogen).

*Immunoprecipitation*

A549 cells were stimulated by TNF-α for 30 minutes before the protein was extracted. Cells were then lyzed with assay buffer [1% (v/v) Nonidet P-40, 0.5 mM EGTA, 5 mM sodium orthovanadate, 10% (v/v) glycerol, 100 μg/mL phenylmethylsulfonyl fluoride, 1 μg/mL leupeptin, 1 μg/mL pepstatin A, 1 μg/mL aprotinin and 50 mM HEPES (pH 7.5)]. Aliquots of 500 μL diluted lysate (1 μg protein/μL) were incubated with the antibody (5 μL) against PPARγ overnight. The immune complex was captured by 1:1 (v/v) protein A-Sepharose 4B bead suspension and incubated for an additional 90 min. The beads were harvested and the proteins bound to them were resolved, separated by SDS-PAGE and analyzed by Western blot.

*Immunohistochemistry*

The tissues were embedded in paraffin after fixation with 4% paraformaldehyde. 4 μm thick sections were prepared, and the sections were blocked with goat serum and then incubated with PPARγ antibody (Abcam, Cambridge, UK) overnight at 4°C. Then the sections were stained with 3,3-diaminobenzidine (DAB) and counterstained with hematoxylin after being incubated with secondary antibody. Both staining intensity and positive percentage were used to examine the expression level of PPARγ in lung cancer tissue: negative =0, weak =1, moderate =2 and strong =3. High PPARγ expression was defined in case of IHC score of 2 or 3 and low PPARγ expression in case of IHC score of 1. Besides, the lung tumor tissues obtained from patients and experimental mouse were stained with antibodies against Ki-67 (Cell Signaling Technology) and HGPRT, separately. All the slides were observed and measured by Olympus microscope (Nikon, Tokyo, Japan).

*Dual-luciferase reporter assay for NF-κB activity*

A549 cells were seeded into 48-well plates in accordance with a density of 50% and were divided into four groups: blank control, GW9662 stimulation, PMX (10 μM) stimulation and PMX (50 μM) stimulation groups. Cells were infected with lentiviral vectors expressing the firefly luciferase gene under the control of NF-κB-responsive elements. The luciferase activity was measured with a LumiStar Optima luminescence counter (BMG Lab Tech, Offenburg, Germany).

*Gene knockdown by lentivirus-delivered short hairpin RNAs*

The short hairpin RNA (shRNA) oligonucleotides were synthesized to target the following sequences of PPARγ: shRNA1, 5'-GACAACAGACAAATCACCATT-3', shRNA2, 5'-AGCATTTCTACTCCACATTA-3', shRNA3, 5'-ATGGAGTCCACGAGATCATTT-3', and the negative control sequence was as follows: 5'-TTCTCCGAACGTGTCACGT-3'. The oligonucleotides were annealed and cloned into pLKO.1-EGFP-Puro (Addgene, Cambridge, USA) and packaged in HEK293T cells. The recombinant lentiviruses were prepared and used for infection of A549 cells. 72 hours later, cells were observed with a fluorescence microscope, and the knockdown efficiency was determined by Western blot.

*Cellular thermal shift assay*

The cellular thermal shift assay was used to investigate thermal stabilization of PPARγ upon PMX incubation. A549 cells were pretreated with PMX 100 ng/ml for 3 hours, and was harvested and washed with PBS supplemented with protease inhibitor cocktail. Cells were suspended with PBS and freeze-thawed twice using liquid nitrogen. The tubes were spun and centrifuged at 20000 g for 20 mins at 4°C. The supernatant was removed from each tube, and the cell lysates were mixed with SDS-PAGE loading buffer. The samples were subject to SDS-PAGE, followed by transfer of separated proteins onto PVDF membrane. The membrane was incubated with the antibody against PPARγ (Cell Signaling Technology), and a HRP-conjugated secondary antibody (DAKO) was used to identify the primary antibodies. The blots were visualized by ECL detection (Invitrogen).

*IL-6 and IL-8 enzyme-linked immunosorbent assay (ELISA)*

IL-6 (ANOGEN, EL 10023) and IL-8 (ANOGEN, EL 10008) in the supernatant of A549 cells treated with 5 ng/ml TNF-α and/or 20 uM PMX were determined by the ELISA kits according to the manufacturer's instructions.

*Animal experiment*

The protocols of all the animal experiments were approved by the Committee for Animal Experimentation of Fourth Military Medical University. Balb/c mice were purchased from the Experimental Animal Center of Fourth Military Medical University. Male mice aged 8 weeks were used in all the experiments. For induction of lung adenocarcinoma model, the animals were given intraperitoneal (i.p.) injection of 1 g/kg/w dose of urethane for 4 weeks, and then the mice in PMX treatment group were injected with PMX 100 mg/kg/w for 24 weeks, compared with i.p. injection with 0.9% NaCl 100 μl/kg/w for 24 weeks in control group. All the animals were sacrificed for histological examination of tumor formation in the lung.

*Histological analysis*

The mouse lung tissues were fixed with 10% formalin and embedded in paraffin. The samples were cut into 4 μm sections and then stained with hematoxylin and eosin at room temperature. Each section was examined under a light microscope to identify the formation of tumor focus.

*Statistical analysis*

Data were presented as mean ± SD and analyzed using one-way analysis of variance. Comparisons between treatment groups were made using two-tailed unpaired or paired Student's t-test. Kaplan-Meier analysis was used to estimate PFS, whereas Log-rank test was used to assess differences. $P<0.05$ was considered as statistically significant. All the statistical analyses were performed using SPSS 19.0 software.

## Results

*PMX suppressed lung cancer cell proliferation in vitro and tumorigenesis in vivo*

The cytotoxicity of PMX, a folate antimetabolite primarily believed to inhibit key enzymes in purine and pyrimidine synthesis, was explored in lung cancer for the first time. As shown in **Figure 1A**, PMX treatment significantly inhibited the growth of lung cancer cell line A549 and PC-9. The antitumor capacity of PMX was evaluated subsequently using urethane-induced mouse lung adenocarcinoma model. Administration of urethane resulted in the formation of multiple lung cancer foci (**Figure 1B**). However, treatment with PMX significantly suppressed the growth of urethane-elicited tumors in mice (**Figure 1C**). Similarly, PMX treatment decreased the ratio of cells expressing Ki-67 (**Figure 1D**). Thus, PMX efficiently suppressed lung tumorigenesis by impairing the proliferation of malignant cells.

*PMX was predicted to functionally associate with PPARγ*

The potential interaction of PMX with other proteins was analyzed in structure and docking studies, which found that PPARγ, a nuclear receptor that governed divergent cellular processes and inhibited malignancy of various cells [18], was a potential binding partner of PMX (data not shown). Indeed, the thermal shift assay showed that PMX could increase the thermal stability of PPARγ in lung cancer cells (**Figure 2A**), suggesting that PMX might exert an anticancer effect partially via association with PPARγ. Although PMX has been found to suppress cell growth via alternative mechanisms, it exerts a cytotoxic effect mainly by targeting enzyme involved in folic acid metabolism and thereby impairing nucleotide synthesis [19]. The expression of PPARγ was knocked down in A549 cell line, which was validated by Western blot (**Figure 2B**). And whether PPARγ regulated the expression of hypoxanthine-guanine phosphoribosyl transferase (HGPRT), a key enzyme for nucleotide salvage synthesis, was then investigated. The Western blot indicated that PPARγ knockdown increased the level of HGPRT, suggesting an inhibitory role of PPARγ in HGPRT (**Figure 2C**).

*PPARγ was correlated with a favorable prognosis of lung cancer*

PPARγ level was detected in the cancer tissue and adjacent tissue from non-squamous NSCLC patients. Of the paired tissues from 4 patients, the cancerous tissues of 2 patients displayed a remarkable downregulation of PPARγ when compared with adjacent normal

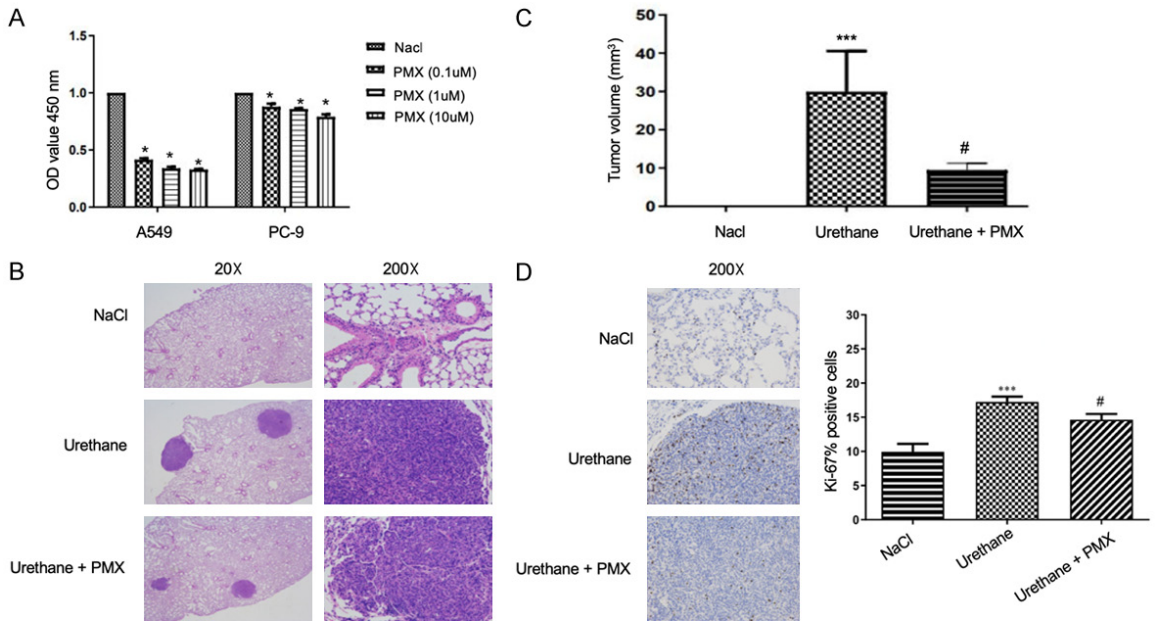


**Figure 1.** PMX suppresses NSCLC cell growth and pulmonary tumorigenesis. (A) NSCLC cells were treated with or without indicated doses of PMX for 48 h, and CCK-8 assays showed that PMX dose-dependently inhibited growth of NSCLC cells. (B-D) Mice were randomly grouped for injection with urethane or NaCl as a control and treatment with or without PMX. The lung tissues were sectioned for haematoxylin and eosin staining (B), and total volumes of tumors developed in each mouse (mean ± SD) were calculated and plotted (C), showing that PMX repressed urethane-induced tumor development. The lung sections were also subject to immunohistochemical staining for Ki-67 (D). **P*<0.001 versus Nacl group. ****P*<0.001 versus Nacl group. #*P*<0.05 versus urethane group.

tissues (**Figure 3A**). The correlation between PPARγ expression and the survival time was further investigated in 44 patients with non-squamous NSCLC. At first, the patients were grouped according to the expression level of PPARγ based on IHC score analysis (1: weak; 2: moderate; and 3: strong) (**Figure 3B**). The survival analysis showed that higher PPARγ expression was related to a longer median progression-free survival (mPFS) in PMX-treated patients (P=0.0005) (**Figure 3C**). In addition, the expression of PPARγ was inversely correlated with HGPRT expression in tumor tissues (**Figure 3D**). These data suggested that the protein level of PPARγ was critically involved in PMX treatment of non-squamous NSCLC patients.

*PMX inhibited NF-κB signaling and lung carcinogenesis through PPARγ*

Whether PMX impaired the growth of lung cancer cells through PPARγ was then probed. PPARγ was highly expressed in lung cancer cell line H520, H1975, SW900, and A549 cells (**Figure 4A**). PPARγ was thus knocked down in A549 cells via lentivirus-delivered shRNAs. As a result, knockdown of PPARγ attenuated the suppression of cell growth by PMX (**Figure 4B**). These data suggested that PMX prevented lung carcinogenesis at least partially through PPARγ. PPARγ was reported to inactivate the NF-κB pathway [20]. In accordance with these reports, it was found that basal and TNF-α-induced phosphorylation of p65 level was significantly enhanced in A549 cell lines after knockdown of PPARγ (**Figure 4C**). Immunoprecipitation assay showed that PPARγ was associated with p65 (**Figure 4D**). These data suggested that PPARγ negatively regulated NF-κB signaling through binding to p65 in lung cancer cells.

*PMX inhibited NF-κB signaling by activating PPARγ*

Whether PMX impeded NF-κB signaling via PPARγ was then explored in lung cancer cells. As expected, PMX treatment inhibited TNF-α-induced activation of NF-κB and ablated the upregulation of the NF-κB target gene, c-Myc [21] (**Figure 5A**). Similarly, PMX suppressed the production of inflammatory factors by untreated cells or those treated with TNF-α (**Figure**

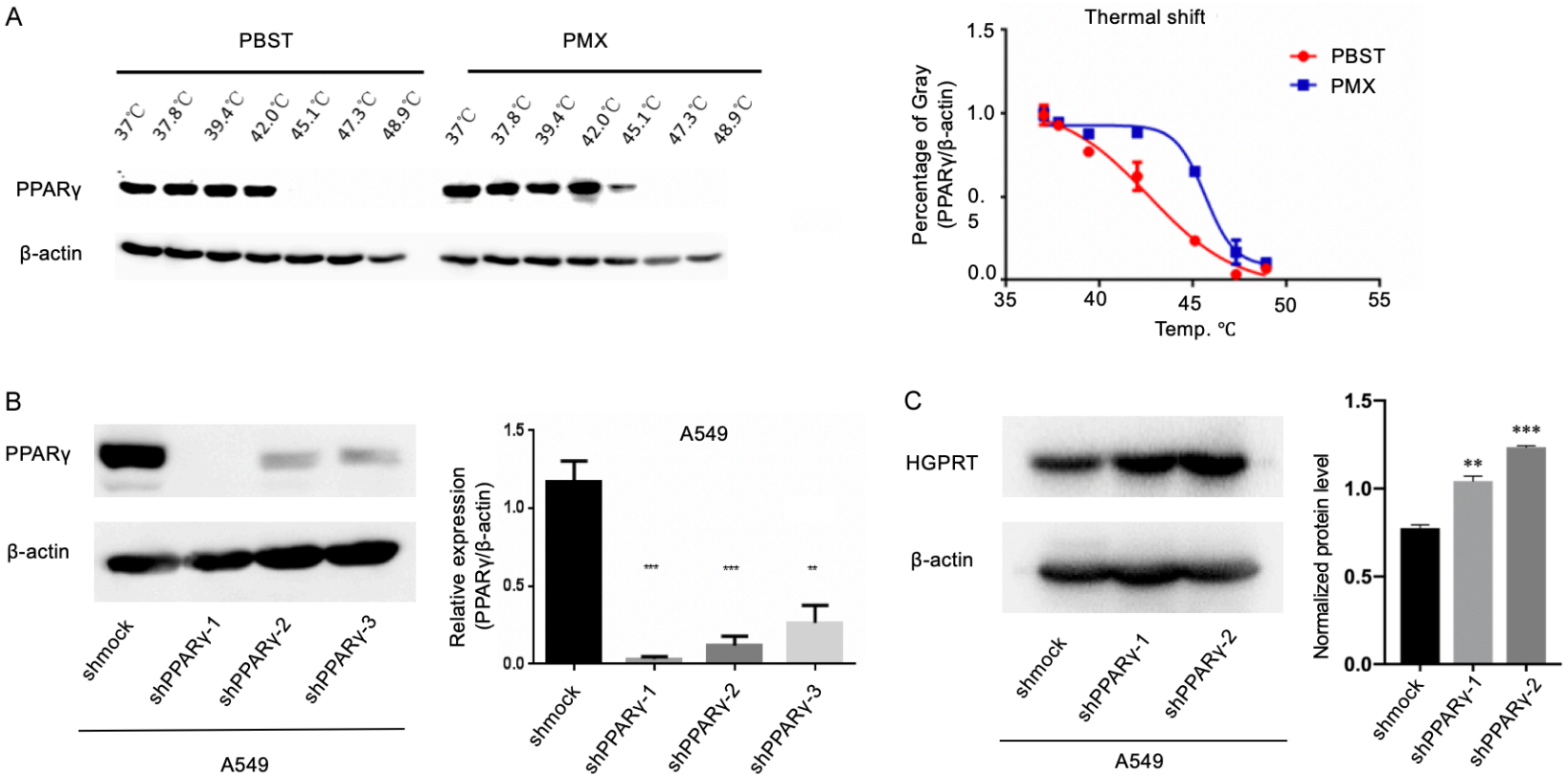


**Figure 2.** PPARγ is functionally associated with PMX in NSCLC cells. A. Thermal shift assay showing increased thermal stability of PMX-incubated PPARγ via Western blot analysis. B and C. A549 cells were infected with lentiviruses expressing control (shMock) or PPARγ-targeted shRNAs, and Western blot analysis showed that PPARγ knockdown increased HGPRT expression in NSCLC cells. ***P*<0.01, ****P*<0.001, compared with shMock.

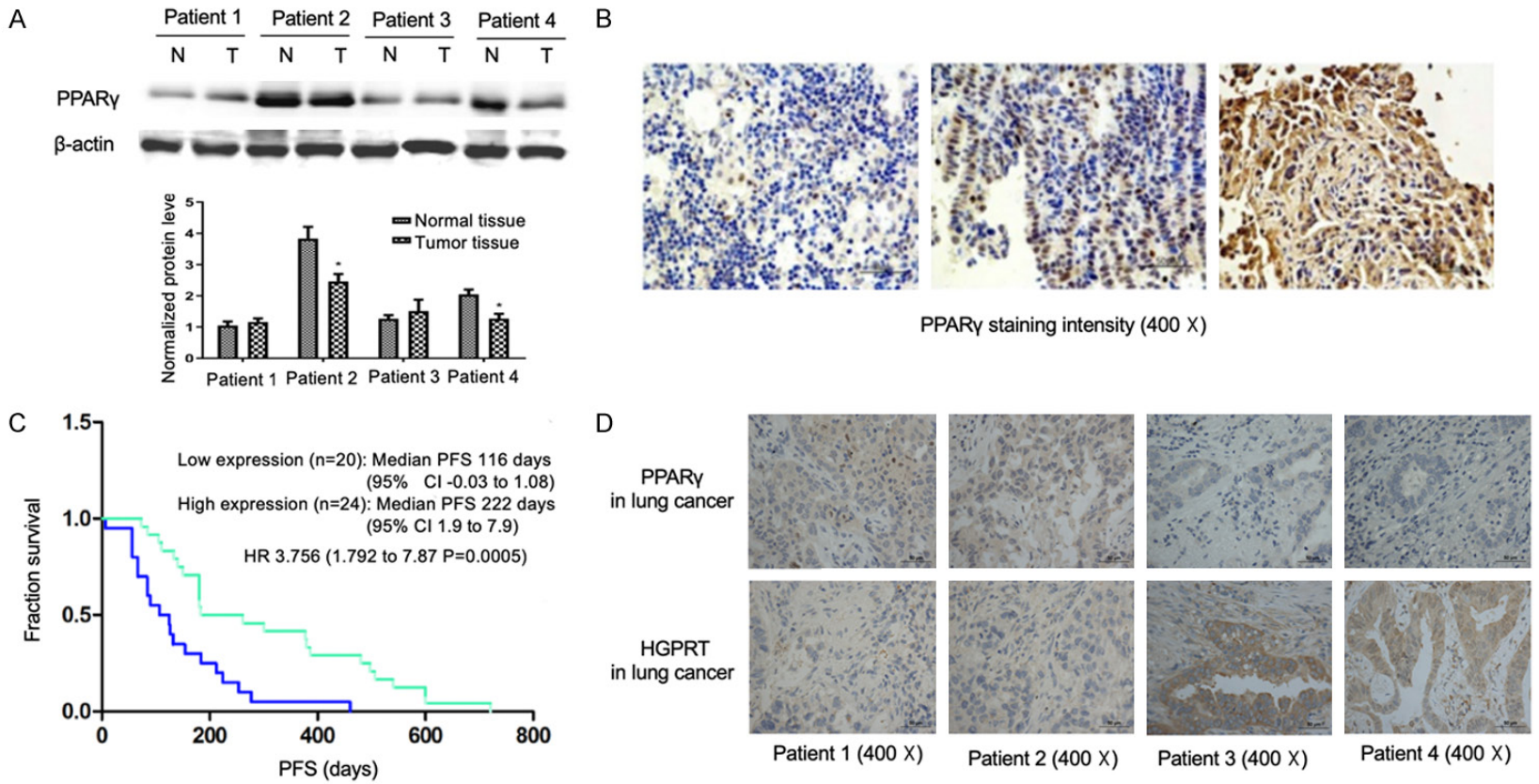


**Figure 3.** PPARγ expression correlates with PFS of NSCLC patients receiving PMX treatment. A. Representative Western Blot images (left) and quantification of 3 independent blottings (right) for PPARγ in cancer tissues of four NSCLC patients. B. Representative IHC staining for PPARγ in NSCLC tissues of different patients with intensities classified as weak (1), moderate (2) and strong (3). C. PFS for NSCLC patients (n=44) expressing high and low PPARγ were plotted, showing that PPARγ expression was associated with prolonged patient survival. D. IHC staining showed that PPARγ and HGPRT expression was inversely correlated in clinical NSCLC tissues. *$P$<0.05 versus normal tissue.

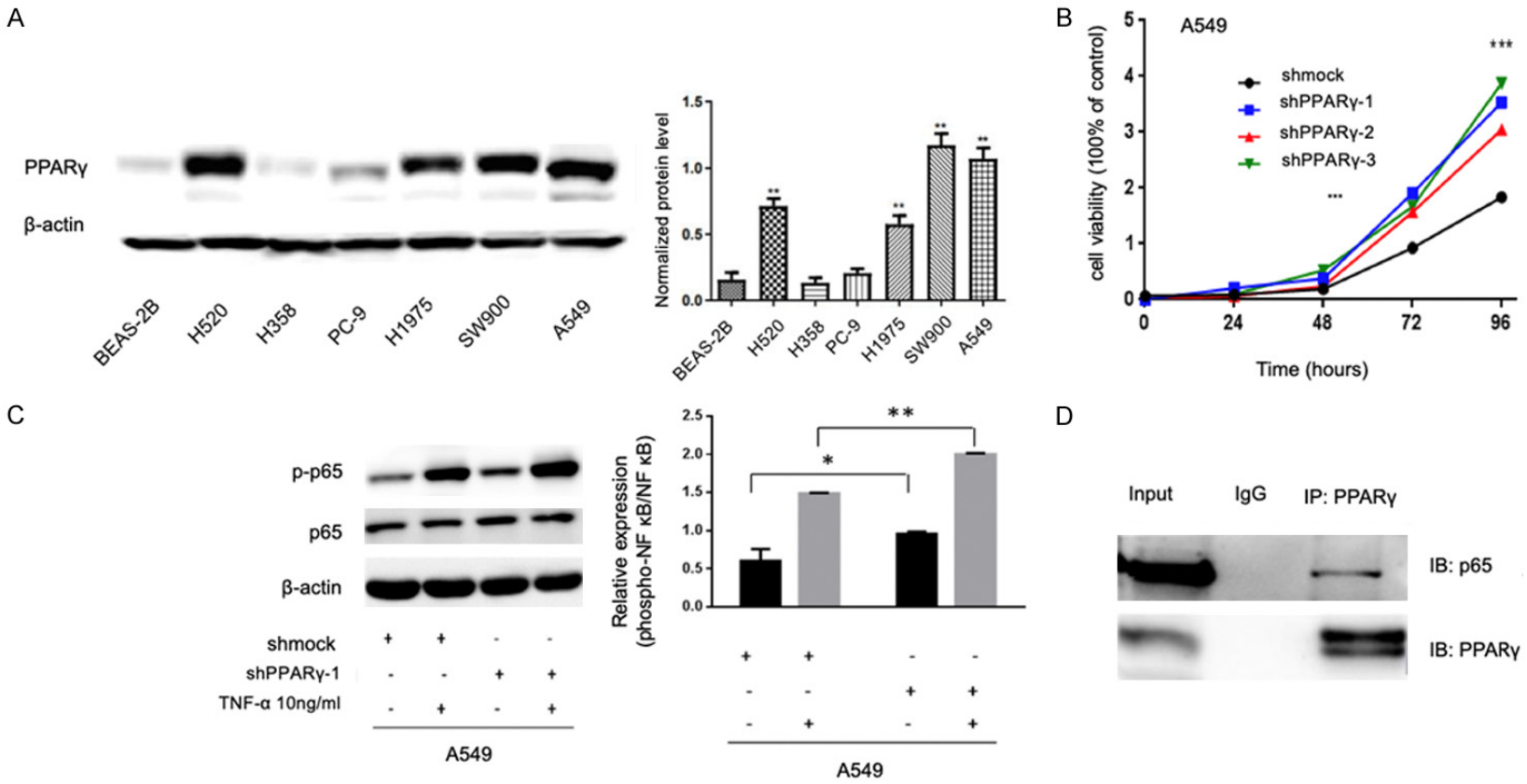


**Figure 4.** PPARγ inhibits the growth and NF-κB activity in NSCLC cells. A. Representative Western Blot images for PPARγ using lysates of indicated bronchial epithelial and NSCLC cell lines. ***P*<0.01 versus BEAS-2B. B. A549 cells were infected with lentiviruses expressing control (shMock) or PPARγ-targeted shRNAs, and the viability of cells was measured via CCK-8 assays showed that expression of these shRNAs increased the viability of NSCLC cells. ****P*<0.001, compared with shMock. C. A549 cells infected with lentiviruses expressing control or PPARγ-targeted shRNAs were treated with TNF-α for 24 hrs, and Western blot analysis showed that PPARγ knockdown facilitated NF-κB p65 activation. The blotting results in 3 independent experiments were quantified and the ratios of p-p65 to p65 were plotted (right). D. Immunoprecipitation using A549 cell lysates was performed, followed by Western blot analysis for the p65 and PPARγ.

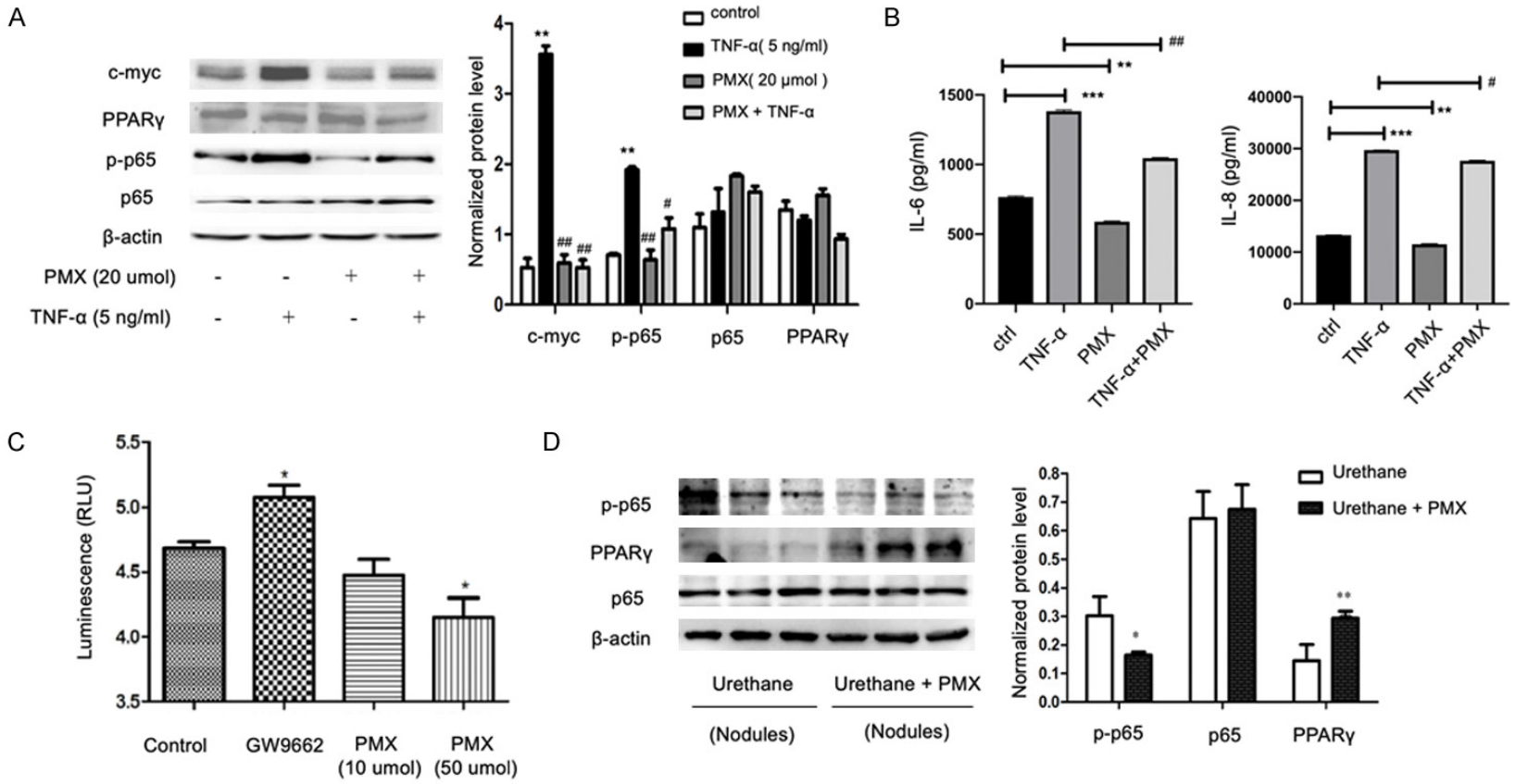


**Figure 5.** PMX impairs NF-κB activity in NSCLC cells and in vivo pulmonary tumors. (A and B) A549 cells were treated with TNF-α and/or PMX for 24 hrs. Western blot analysis indicated that PMX impaired NF-κB activation (A, ***P*<0.01, compared with control group; ##*P*<0.01, #*P*<0.05, compared with TNF-α group), and ELISA using the media of cultured cells showed suppressed inflammatory cytokine production by PMX (B, ****P*<0.001, ***P*<0.01, compared with control group; ##*P*<0.01, #*P*<0.05, compared with TNF-α group). (C) A549 cells were transfected with a luciferase reporter vector harboring the responsive elements of NF-κB, and were treated as indicated. Cells were then subject to assays for luciferase activities, which indicated that PMX inhibited transcriptional activity of NF-κB (C, **P*<0.05, compared with the control group). (D) In urethane induced lung tumorigenesis mice model, tumor nodules in the lung were isolated and subject to Western blot analysis (left), showing that PMX treatment upregulated PPARγ and attenuated NF-κB activation. The blotting results in 3 independent experiments were quantified and plotted (right). **P*<0.05, ***P*<0.01, compared with the urethane group.

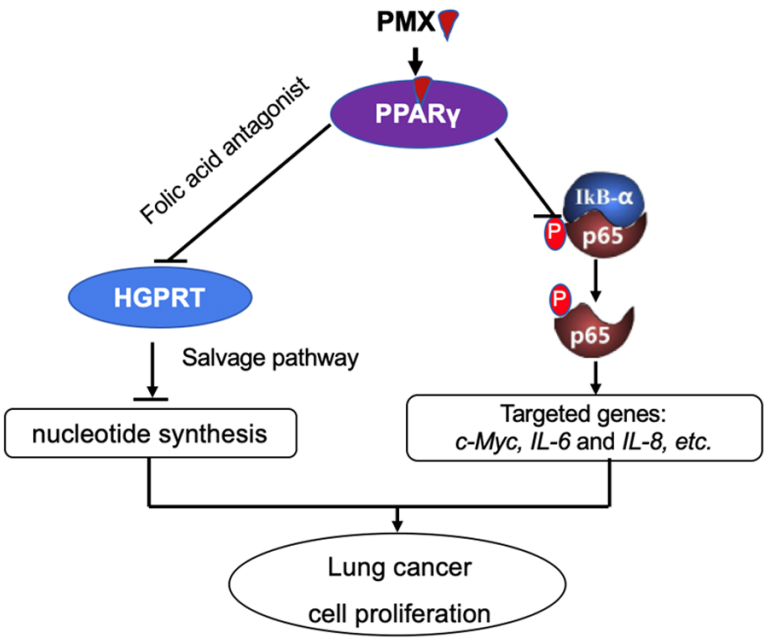


**Figure 6.** Schematic diagram of PPARγ-mediated anti-tumor effect of PMX in NSCLC. The downregulation of HGPRT by PPARγ impairs nucleotide synthesis in a salvage pathway, thereby sensitizing NSCLC cells to PMX inhibition of nucleotide de novo synthesis. In addition, as a candidate partial agonist of PPARγ, PMX actives PPARγ, which binds to NF-κB and transcriptionally suppresses the NF-κB targeted gene, *c-Myc*.

**5B**). A luciferase reporter assay confirmed a marked inhibition on NF-κB transcriptional activity by PMX in lung cancer cells, while NF-κB transcriptional activity was increased upon treatment with GW9662, a PPARγ antagonist (**Figure 5C**). PMX treatment also reduced the activation of NF-κB and increased the protein level of PPARγ in urethane-induced pulmonary tumor nodules in mice (**Figure 5D**). Therefore, PMX exerted a suppressive role in lung tumorigenesis probably via PPARγ-mediated inhibition on NF-κB pathway.

## Discussion

The present study sought to identify intracellular mediators of the therapeutic efficacy of PMX in NSCLC patients. Using lung cancer cell lines and urethane-induced lung adenocarcinoma model, it was found that the expression level of PPARγ was positively correlated with the antitumor activity of PMX. Our results indicated that PMX and PPARγ suppressed the salvage pathway of nucleotide synthesis, in addition to the inhibition on the de novo pathway of nucleotide synthesis. It was also found that as a PPARγ agonist, PMX could activate PPARγ to inhibit NF-κB activity, thereby counteracting the proliferation of lung cancer cells (**Figure 6**).

PMX is a multi-target antifolate drug that has been approved for the first-line treatment of advanced non-squamous NSCLC [22]. The underlying mechanism involves the inhibition on three key enzymes in folate metabolic pathway: thymidylate synthase (TYMS), dihydrofolate reductase (DHFR), and glycinamide ribonucleotide formyltransferase (GARFT) [5]. Remarkably, the sensitivity and efficiency of PMX treatment vary in different patients. Due to the lack of biomarkers to predict the outcome of PMX treatment, it is difficult to determine which patients are more suitable for PMX treatment and what adjuvant therapy can be applied to improve the efficacy [7]. Peroxisome proliferators-activated receptors (PPARs) are members of the nuclear receptor superfamily of ligand-dependent transcription factors [23]. Of the 3 subtypes, PPARγ plays an important role in the regulation of various functions, such as lipid homeostasis, adipocyte differentiation, inflammation, and cancer biology [23]. PPARγ has been shown to be expressed in several human tumors, including lung cancer [24]. In the present study, it was found that PPARγ was expressed in human lung cancer cells and tissues, although the expression level varied in different patients and cell lines. Cumulative evidence has demonstrated the anti-proliferative and pro-apoptotic effects of PPARγ agonists, suggesting that PPARγ could be considered as a potential target for the treatment of cancer [25, 26]. Moreover, previous studies have revealed that activating PPARγ was a novel chemopreventive strategy for cancers [13]. In this study, it was found that higher level of PPARγ was correlated with a longer PFS in non-squamous NSCLC patients receiving PMX treatment. Notably, with the aid of explicit solvent molecular dynamics simulations, PPARγ was demonstrated as a key mediator of chemotherapy with PMX, and that PMX

might function as a partial agonist of PPARγ. These findings are in line with the established tumor-suppressive role of PPARγ in various malignancies and with the multifaceted cellular effect of PMX in addition to the inhibition on folate metabolism.

In eukaryocytes, nucleotides are synthesized via de novo or salvage pathway. The cytotoxicity of PMX relies largely on its capability to suppress de novo nucleotide synthesis [27]. Our finding that PPARγ downregulated HGPRT suggested that PPARγ might sensitize cells to PMX suppression of de novo nucleotide synthesis through blocking the salvage purine synthetic pathway. Nuclear factor-κB (NF-κB) is a key transcription factor that substantially regulates gene transcription and cell survival [28, 29]. The activation of NF-κB is a crucial contributor in the progression of various malignancies [30]. Several reports have found higher NF-κB protein levels in cancer tissues compared to normal tissues [31, 32]. Here, it was found that PMX could impair NF-κB phosphorylation through activating PPARγ both in vitro and in vivo. Given the critical involvement of chronic inflammation in carcinogenesis and the role of NF-κB in switching on inflammatory factor genes, it is worth further investigation on whether PMX prevents the occurrence of NSCLC by targeting NF-κB pathway.

To the best of our knowledge, this is the first study to show that the expression of PPARγ is positively correlated with the anticancer activity of PMX. In addition, our results supported the proposal that PMX could activate PPARγ to inhibit NK-κB activity and suppress the malignant behaviors of lung cancer cells. However, there are some limitations in our study. Firstly, the sample size is relatively small in the prognosis analysis. Secondly, the conformational basis and the outcome of PPARγ binding with PMX need to be further investigated. Nevertheless, our findings provide new insights into the antitumor mechanisms of PMX and may pave avenues for the development of additional efficient therapies for lung cancer.

## Acknowledgements

This work was supported by the National Natural Science Foundation of China (Nos. 81670045, 81272586, 81470249 and 81970048) and National Major Science and Technology Projects of China (No. 2018ZX09711002).

## Disclosure of conflict of interest

None.

**Address correspondence to:** Shengqing Li, Department of Pulmonary and Critical Care Medicine, Huashan Hospital, Fudan University, Shanghai 200040, China. E-mail: shengqingli@hotmail.com

## References

[1] Hoffman PC, Mauer AM and Vokes EE. Lung cancer. Lancet 2000; 355: 479-485.

[2] Goldstraw P, Ball D, Jett JR, Le Chevalier T, Lim E, Nicholson AG and Shepherd FA. Non-small-cell lung cancer. Lancet 2011; 378: 1727-1740.

[3] Paz-Ares L and Corral J. Treatment for early-stage lung cancer: what next? Lancet 2014; 383: 1528-1530.

[4] Rossi A, Ricciardi S, Maione P, de Marinis F and Gridelli C. Pemetrexed in the treatment of advanced non-squamous lung cancer. Lung Cancer 2009; 66: 141-149.

[5] Shih C, Chen VJ, Gossett LS, Gates SB, MacKellar WC, Habeck LL, Shackelford KA, Mendelsohn LG, Soose DJ, Patel VF, Andis SL, Bewley JR, Rayl EA, Moroson BA, Beardsley GP, Kohler W, Ratnam M and Schultz RM. LY231514, a pyrrolo[2,3-d]pyrimidine-based antifolate that inhibits multiple folate-requiring enzymes. Cancer Res 1997; 57: 1116-1123.

[6] Cohen MH, Justice R and Pazdur R. Approval summary: pemetrexed in the initial treatment of advanced/metastatic non-small cell lung cancer. Oncologist 2009; 14: 930-935.

[7] Rossi G, Alama A, Genova C, Rijavec E, Tagliamento M, Biello F, Coco S, Dal Bello MG, Boccardo S and Grossi F. The evolving role of pemetrexed disodium for the treatment of non-small cell lung cancer. Expert Opin Pharmacother 2018; 19: 1969-1976.

[8] Niyikiza C, Baker SD, Seitz DE, Walling JM, Nelson K, Rusthoven JJ, Stabler SP, Paoletti P, Calvert AH and Allen RH. Homocysteine and methylmalonic acid: markers to predict and avoid toxicity from pemetrexed therapy. Mol Cancer Ther 2002; 1: 545-552.

[9] Szabo E. Selecting targets for cancer prevention: where do we go from here? Nat Rev Cancer 2006; 6: 867-874.

[10] Gampe RT Jr, Montana VG, Lambert MH, Miller AB, Bledsoe RK, Milburn MV, Kliewer SA, Willson TM and Xu HE. Asymmetry in the PPARgamma/RXRalpha crystal structure reveals the molecular basis of heterodimerization among nuclear receptors. Mol Cell 2000; 5: 545-555.

[11] Liu Y, Yan X, Mao G, Fang L, Zhao B, Liu Y, Tang H and Wang N. Metabonomic profiling revealed an alteration in purine nucleotide metabolism

associated with cardiac hypertrophy in rats treated with thiazolidinediones. J Proteome Res 2013; 12: 5634-5641.
[12] Nemenoff RA, Weiser-Evans M and Winn RA. Activation and molecular targets of peroxisome proliferator-activated receptor-gamma ligands in lung cancer. PPAR Res 2008; 2008: 156875.
[13] Ondrey F. Peroxisome proliferator-activated receptor gamma pathway targeting in carcinogenesis: implications for chemoprevention. Clin Cancer Res 2009; 15: 2-8.
[14] Keith RL and Miller YE. Lung cancer chemoprevention: current status and future prospects. Nat Rev Clin Oncol 2013; 10: 334-343.
[15] Nissen SE and Wolski K. Effect of rosiglitazone on the risk of myocardial infarction and death from cardiovascular causes. N Engl J Med 2007; 356: 2457-2471.
[16] Burgermeister E, Schnoebelen A, Flament A, Benz J, Stihle M, Gsell B, Rufer A, Ruf A, Kuhn B, Marki HP, Mizrahi J, Sebokova E, Niesor E and Meyer M. A novel partial agonist of peroxisome proliferator-activated receptor-gamma (PPARgamma) recruits PPARgamma-coactivator-1alpha, prevents triglyceride accumulation, and potentiates insulin signaling in vitro. Mol Endocrinol 2006; 20: 809-830.
[17] Montanari R, Saccoccia F, Scotti E, Crestani M, Godio C, Gilardi F, Loiodice F, Fracchiolla G, Laghezza A, Tortorella P, Lavecchia A, Novellino E, Mazza F, Aschi M and Pochetti G. Crystal structure of the peroxisome proliferator-activated receptor gamma (PPARgamma) ligand binding domain complexed with a novel partial agonist: a new region of the hydrophobic pocket could be exploited for drug design. J Med Chem 2008; 51: 7768-7776.
[18] Shafi S, Gupta P, Khatik GL and Gupta J. PPARgamma: potential therapeutic target for ailments beyond diabetes and its natural agonism. Curr Drug Targets 2019; 20: 1281-1294.
[19] Severi L, Losi L, Fonda S, Taddia L, Gozzi G, Marverti G, Magni F, Chinello C, Stella M, Sheouli J, Braicu EI, Genovese F, Lauriola A, Marraccini C, Gualandi A, D'Arca D, Ferrari S and Costi MP. Proteomic and bioinformatic studies for the characterization of response to pemetrexed in platinum drug resistant ovarian cancer. Front Pharmacol 2018; 9: 454.
[20] Ruan H, Pownall HJ and Lodish HF. Troglitazone antagonizes tumor necrosis factor-alpha-induced reprogramming of adipocyte gene expression by inhibiting the transcriptional regulatory functions of NF-kappaB. J Biol Chem 2003; 278: 28181-28192.
[21] Grumont R, Lock P, Mollinari M, Shannon FM, Moore A and Gerondakis S. The mitogen-induced increase in T cell size involves PKC and NFAT activation of Rel/NF-kappaB-dependent c-myc expression. Immunity 2004; 21: 19-30.
[22] Baldwin CM and Perry CM. Pemetrexed: a review of its use in the management of advanced non-squamous non-small cell lung cancer. Drugs 2009; 69: 2279-2302.
[23] Clark RB. The role of PPARs in inflammation and immunity. J Leukoc Biol 2002; 71: 388-400.
[24] Elstner E, Muller C, Koshizuka K, Williamson EA, Park D, Asou H, Shintaku P, Said JW, Heber D and Koeffler HP. Ligands for peroxisome proliferator-activated receptorgamma and retinoic acid receptor inhibit growth and induce apoptosis of human breast cancer cells in vitro and in BNX mice. Proc Natl Acad Sci U S A 1998; 95: 8806-8811.
[25] Shen B, Chu ES, Zhao G, Man K, Wu CW, Cheng JT, Li G, Nie Y, Lo CM, Teoh N, Farrell GC, Sung JJ and Yu J. PPARgamma inhibits hepatocellular carcinoma metastases in vitro and in mice. Br J Cancer 2012; 106: 1486-1494.
[26] Cao LQ, Shao ZL, Liang HH, Zhang DW, Yang XW, Jiang XF and Xue P. Activation of peroxisome proliferator-activated receptor-gamma (PPARgamma) inhibits hepatoma cell growth via downregulation of SEPT2 expression. Cancer Lett 2015; 359: 127-135.
[27] Roy B, Depaix A, Perigaud C and Peyrottes S. Recent trends in nucleotide synthesis. Chem Rev 2016; 116: 7854-7897.
[28] Hoesel B and Schmid JA. The complexity of NF-kappaB signaling in inflammation and cancer. Mol Cancer 2013; 12: 86.
[29] Ben-Neriah Y and Karin M. Inflammation meets cancer, with NF-kappaB as the matchmaker. Nat Immunol 2011; 12: 715-723.
[30] DiDonato JA, Mercurio F and Karin M. NF-kappaB and the link between inflammation and cancer. Immunol Rev 2012; 246: 379-400.
[31] Lewander A, Gao J, Adell G, Zhang H and Sun XF. Expression of NF-kappaB p65 phosphorylated at serine-536 in rectal cancer with or without preoperative radiotherapy. Radiol Oncol 2011; 45: 279-284.
[32] Abdullah M, Rani AA, Sudoyo AW, Makmun D, Handjari DR and Hernowo BS. Expression of NF-kB and COX2 in colorectal cancer among native Indonesians: the role of inflammation in colorectal carcinogenesis. Acta Med Indones 2013; 45: 187-192.